Damping Performance Improvement for PV-Integrated Power Grids via Retrofit Control

Hampei Sasahara[a,1], Takayuki Ishizaki[a], Tomonori Sadamoto[a], Taisuke Masuta[b], Yuzuru Ueda[c], Hideharu Sugihara[d], Nobuyuki Yamaguchi[c], Jun-ichi Imura[a]

[a] *Graduate School of Engineering, Tokyo Institute of Technology, 2-12-1, O-okayama, Meguro-ku, Tokyo 152-8552, Japan.*
[b] *Graduate School of Science and Technology, Meijo University, 1-501, Shiogamaguchi, Tempaku-ku, Nagoya, Aichi 468-8502, Japan.*
[c] *Graduate School of Engineering, Tokyo University of Science, 6-3-1, Niijuku, Katsushika-ku, Tokyo 125-8585, Japan.*
[d] *Graduate School of Engineering, Osaka University, 1-1, Yamadaoka, Suita, Osaka 565-0871, Japan.*

Abstract

In this paper, we develop a distributed design method for power system stabilizers (PSSs) that improve damping performance for deflections caused by contingencies in a power grid in which large-scale PV penetration is introduced. We suppose that there are multiple independent system operators in a grid and each system operator designs a PSS based on the corresponding subsystem model information alone. The controller design method for PSSs under the restriction on available model information is called distributed design. Although practical distributed design methods are typically based on single-machine infinite-bus system, the problem here is that the designed controller possibly destabilizes the grid. In this paper, we propose a novel distributed design method for power grids based on retrofit control theory. The designed PSS can theoretically guarantee the stability of power grids and also improves damping performance. Through a numerical example for the IEEJ EAST 30-machine power system, the effectiveness of our proposed method is verified compared with the conventional method.

Keywords: Distributed design, Large-scale systems, Power systems, Retrofit control, Smart grid

1. Introduction

Towards development of smart grids, the use of renewable power generation systems such as photovoltaic (PV) generators has become increasingly popular [Blaabjerg et al. (2017)]. In Japan, the number of installed PV power generators is rapidly growing after the implementation of the feed-in tariff (FIT) scheme [Ministry of Economy, Trade, and Industry (2017a)], and the cumulative level of PV installations is expected to reach 64GW by 2030, covering approximately 7% of the entire energy consumption [Ministry of Economy, Trade, and Industry (2015)]. Such large-scale penetration of PV generators possibly causes the operation stoppage of some pre-existing synchronous generators in order to keep supply-demand balance. In [Eftekharnejad et al. (2013); Tamimi et al. (2013); Blaabjerg et al. (2006)], it has been pointed out that the reduction of the number of pre-existing generators poses a threat to power system stability because the poor controllability of PV leads to grid instability [Blaabjerg et al. (2004)]. From this viewpoint, it is required to develop a systematic method for designing power system stabilizers (PSSs) that can enhance the stability of PV-integrated power systems.

One approach to this objective would be to use distributed control [Etemadi et al. (2012), Ortega et al. (2005), Dörfler et al. (2014)], where each local control action is determined only by local measurement output, such as local frequency deviation. Although in the above PSS design, all the controllers are jointly designed with access to a model of the entire system, it is impossible to obtain the entire power system model because power systems are highly large-scale and complex. Therefore, this type of entire-model-based approach is not very suitable for the control of power systems.

Recently, a new notion called *distributed design* has been proposed [Langbort and Delvenne (2010)]. This notion is the controller design in which local controllers are individually designed by using partial models of the entire system and their control actions are individually determined by local feedback from the corresponding subsystems. In other words, not only the controllers' action, but also their design is performed for individual subsystems. Hence, this distributed design approach is suitable for the control of large-scale systems. Indeed, typical controller design approaches taken in the power community

[1] FAX: +81-3-5734-3635, email: sasahara.h@cyb.sc.e.titech.ac.jp.

can be regarded as special cases of this distributed design. Such an example is PSS design based on the single-machine infinite-bus model in which the dynamical behavior of the grid is completely neglected [Wang and Swift (1997)]. However, such typical PSS design does not theoretically guarantee the stability of the entire power system. Although existing power grids are stably operated by conventional PSSs, especially for future power grids PSS design should take an approach based on distributed design methods that can guarantee the entire system stability theoretically.

As a practical distributed design method, the authors in [Ishizaki et al. (2018)] have proposed a new control concept, *retrofit control*. The target system of retrofit control is a network system in which there are multiple operators each of who manages the corresponding subsystem using a local controller so that the entire system is stable. Consider a situation where operators attempt to retrofit an additional controller to the network for transient response improvement. The proposed retrofit control enables the operators to achieve distributed design.

In this paper, we show how retrofit control works for PSS design of PV-integrated power grids. The existing method in [Ishizaki et al. (2018)], however, treats the systems where feedthrough terms from interconnection signals to measurement signals do not exist and thus cannot be applied to power systems directly. To overcome this difficulty, we extend the existing retrofit control so as to be applicable for power systems. We see numerically that the proposed approach effectively works for enhancing damping performance of the controlled grid.

This paper builds on the preliminary version [Sasahara et al. (2017)], where we have introduced the fundamental idea of retrofit control for power systems. While PV is not considered in the system treated in [Sasahara et al. (2017)], we introduce PV plants and consider PSS design for PV-integrated power systems. Further, this paper provides rigorous theory of retrofit control that realizes distributed design for power systems. The numerical simulation here is performed for a more realistic power system model than the model used in our conference paper [Sasahara et al. (2017)].

The remainder of this paper is organized as follows. In Section 2, we describe a state-space model of the electric power system. In Section 3, we mathematically formulate the controller design problem. Moreover, we propose a distributed design method for local controllers based on retrofit control. To demonstrate the effectiveness of our proposed method, numerical simulation for PV-integrated IEEJ EAST 30-machine power system [The Institute of Electrical Engineers of Japan Power and Energy (2016)], called EAST30 model for short, is shown in Section 4. Section 5 draws conclusion.

Notation. We denote the set of real numbers by $\mathbb{R}$, the set of complex numbers by $\mathbb{C}$, the identity matrix by $\mathbf{I}$, the transpose of a vector $\mathbf{x}$ and a matrix $\mathbf{A}$ by $\mathbf{x}^\mathsf{T}$ and $\mathbf{A}^\mathsf{T}$, respectively, the spectrum of a matrix $\mathbf{A}$ by $\sigma(\mathbf{A})$, the Euclidean norm of a vector $\mathbf{x}$ by $\|\mathbf{x}\|$, the 2-induced norm of a matrix $\mathbf{A}$ by $\|\mathbf{A}\|$, the vector where $\mathbf{x}, \mathbf{y}$ and $\mathbf{x}_i,\ i \in \mathcal{I}$ are arranged in vertical by $\mathrm{col}(\mathbf{x}, \mathbf{y})$ and $\mathrm{col}(\mathbf{x}_i)_{i\in\mathcal{I}}$, respectively, and the cardinality of a set $\mathcal{I}$ by $|\mathcal{I}|$. The complex variables are described in bold italic fonts, e.g., $\boldsymbol{x}$. The imaginary unit is denoted by $\boldsymbol{j} := \sqrt{-1}$, the conjugate of $\boldsymbol{x}$ by $\boldsymbol{x}^*$, the absolute value of $\boldsymbol{x}$ by $|\boldsymbol{x}|$, the angle of $\boldsymbol{x}$ by $\angle\boldsymbol{x}$, and the real (imaginary) value of $\boldsymbol{x}$ by $\mathrm{Re}\ \boldsymbol{x}$ ($\mathrm{Im}\ \boldsymbol{x}$). Denote the $\mathcal{L}_2$-norm of a square-integrable function $\mathbf{f}(t)$ by

$$\|\mathbf{f}(t)\|_{\mathcal{L}_2} := \sqrt{\int_0^\infty \|\mathbf{f}(t)\|^2 dt},$$

and the $\mathcal{H}_2$-norm and the $\mathcal{H}_\infty$-norm of a transfer matrix $\mathbf{G}(s)$ by

$$\|\mathbf{G}(s)\|_{\mathcal{H}_2} := \sqrt{\frac{1}{2\pi}\int_{-\infty}^{\infty} \mathrm{tr}\left(\mathbf{G}(\boldsymbol{j}\omega)\mathbf{G}(\boldsymbol{j}\omega)^\mathsf{T}\right) d\omega}$$

and

$$\|\mathbf{G}(s)\|_{\mathcal{H}_\infty} := \sup_{\omega\in\mathbb{R}} \|\mathbf{G}(\boldsymbol{j}\omega)\|,$$

respectively. Throughout the paper, all physical quantities, e.g., the rotor angular speed ω, are in per unit unless otherwise stated, and all symbols with superscript $\star$ denote setpoints, e.g., $\boldsymbol{V}^\star$ is the setpoint of $\boldsymbol{V}$.

2. Modeling of PV-integrated Power Systems

We first describe a state-space model of an electric power system consisting of power plants, consumers, PV generators, and transmission facilities of the EAST30 model [The Institute of Electrical Engineers of Japan Power and Energy (2016)]. In the modeling, neighboring power plants, consumers, and PV generators are considered to be aggregated ones called generator, load, and PV power plant, respectively. Those aggregated units are interconnected via buses. In this paper, the term non-unit buses refers to the buses to which any units are not attached, and the term component refers to either a unit with its bus or the non-unit bus.

Let N be the number of the buses existing in the power system. For $k \in \mathbb{N}$ where $\mathbb{N} := \{1, \dots, N\}$, the dynamics of the k-th component is described as

$$\Sigma_{[k]} : \begin{cases} \dot{\mathbf{x}}_{[k]} = \mathbf{f}_{[k]}(\mathbf{x}_{[k]}, \boldsymbol{v}_{[k]}, \boldsymbol{i}_{[k]}, u_{\mathrm{s},[k]}, u_{[k]}) \\ 0 \ = \mathbf{g}_{[k]}(\mathbf{x}_{[k]}, \boldsymbol{v}_{[k]}, \boldsymbol{i}_{[k]}) \end{cases} \tag{1}$$

where $x_{[k]}$ is the state of the k-th component, $u_{\mathrm{s},[k]}$ is the supplementary control input defined below, $u_{[k]}$ is the control input, and $\boldsymbol{i}_{[k]}$ and $\boldsymbol{v}_{[k]}$ are the bus current and voltage, respectively.

The interconnection of the network of the power system is described by

$$\boldsymbol{i} = \boldsymbol{Y}\boldsymbol{v} \tag{2}$$

where $\boldsymbol{i} := \mathrm{col}(\boldsymbol{i}_{[i]})_{i\in\mathbb{N}}, \boldsymbol{v} := \mathrm{col}(\boldsymbol{v}_{[i]})_{i\in\mathbb{N}}$, and $\boldsymbol{Y} \in \mathbb{C}^{N\times N}$ is the admittance matrix. It should be emphasized that $\boldsymbol{Y}$ represents the network structure of the power grid.

The entire power system model can be described as the combination of (1) and (2). The remainder of this section is devoted to present models of generators, loads, PV power plants, and non-unit buses in the form of (1). In the following, the index set of the buses connecting to the generators, loads, PV power plants, and non-unit buses are denoted by $\mathbb{N}_\mathrm{G}, \mathbb{N}_\mathrm{L}, \mathbb{N}_\mathrm{P}$, and $\mathbb{N}_\mathrm{N}$, respectively. Those sets are disjoint and $\mathbb{N}_\mathrm{G} \cup \mathbb{N}_\mathrm{L} \cup \mathbb{N}_\mathrm{P} \cup \mathbb{N}_\mathrm{N} = \mathbb{N}$ holds.

2.1. Synchronous Generator

We describe a generator model of the EAST30 model in the form of (1). Typically, a generator consists of a synchronous machine, an excitation system with automatic voltage regulator (AVR), and a turbine with governor [Kundur (1994)]. The basic function of the excitation system is to provide current to the synchronous machine, that of the turbine with governor is to generate a mechanical power to rotate the machine, and the synchronous machine is in charged of changing the mechanical power to the electrical power and transmits the generated mechanical power to the grid.

For $k \in \mathbb{N}_\mathrm{G}$, the dynamics of the synchronous machine connecting to the k-th bus is described as

$$\left\{\begin{array}{ll} \dot{\delta}_{[k]} &= \overline{\omega}\omega_{[k]} \\ \dot{\omega}_{[k]} &= \dfrac{1}{M_{[k]}}\left(\dfrac{1}{1+\omega_{[k]}}P_{\mathrm{m},[k]} - \mathbf{v}_{[k]}^\mathsf{T}\mathbf{i}_{[k]}\right) \\ \dot{\boldsymbol{\psi}}_{[k]} &= \mathbf{A}_{\boldsymbol{\psi}[k]}\boldsymbol{\psi}_{[k]} + \mathbf{B}_{\boldsymbol{\psi}[k]}\mathbf{i}_{[k]} + \mathbf{B}_{V[k]}V_{\mathrm{fd},[k]} \quad , \quad k \in \mathbb{N}_\mathrm{G} \\ \mathbf{v}_{[k]} &= \mathbf{C}_{\boldsymbol{\psi}[k]}\boldsymbol{\psi}_{[k]} + \mathbf{D}_{\boldsymbol{\psi}[k]}\mathbf{i}_{[k]} \\ \boldsymbol{v}_{[k]} &= \mathbf{comp}(\mathbf{T}_{\delta_{[k]}}\mathbf{v}_{[k]}) \\ \boldsymbol{i}_{[k]} &= \mathbf{comp}(\mathbf{T}_{\delta_{[k]}}^{-1}\mathbf{i}_{[k]}) \end{array}\right. \tag{3}$$

where $\delta_{[k]}$ is the rotor angle relative to the frame rotating at the constant reference speed $\overline{\omega} := 100\pi$ (rad/sec), $\omega_{[k]}$ is the rotor angular velocity relative to $\overline{\omega}$, $\psi_{[k]}$ includes the magnetic flux associated with the field circuit, d-axis damper windings, q-axis damper windings, $P_{\mathrm{m},[k]}$ is the mechanical power input, $V_{\mathrm{fd},[k]}$ is the field voltage, and $\mathbf{i}_{[k]}$ and $\mathbf{v}_{[k]}$ are the stator current and the stator voltage, respectively. The inertia constant is denoted by $M_{[k]}$ (sec) and $\mathbf{comp}(\cdot)$ denotes the transformation from a two-dimensional real vector to the corresponding complex number by $\mathbf{comp}(\mathbf{z}) := [1\ \boldsymbol{j}]\mathbf{z}$. Furthermore, $\mathbf{T}_{\delta_{[k]}}$ is defined by

$$\mathbf{T}_{\delta_{[k]}} := \begin{bmatrix} \sin\delta_{[k]} & \cos\delta_{[k]} \\ -\cos\delta_{[k]} & \sin\delta_{[k]} \end{bmatrix}$$

that represents the coordinate transformation matrix from the coordinate system rotating at each generator's own frequency to the coordinate system rotating at the rated frequency. Note that the dynamics (3) corresponds to the coordinate system that rotates at the rotational speed $\omega_{[k]}$.

The dynamics of the turbine with governor is described as

$$\left\{\begin{array}{ll} \dot{\boldsymbol{\zeta}}_{[k]} &= \mathbf{A}_{\boldsymbol{\zeta}[k]}\boldsymbol{\zeta}_{[k]} + \mathbf{B}_{\boldsymbol{\zeta}[k]}\omega_{[k]} + \mathbf{R}_{\boldsymbol{\zeta}[k]}(P^\star_{\mathrm{m},[k]} + u_{\mathrm{s},[k]}) \\ P_{\mathrm{m},[k]} &= \mathbf{C}_{\boldsymbol{\zeta}[k]}\boldsymbol{\zeta}_{[k]} \end{array}\right. \tag{4}$$

where $\boldsymbol{\zeta}_{[k]} \in \mathbb{R}^4$ is the state of the turbine with governor, $P^\star_{\mathrm{m},[k]}$ is the mechanical power in the steady state, and $u_{\mathrm{s},[k]}$ denotes the supplementary generation control action under automatic generation control (AGC) [Kundur (1994)]. Employing AGC, we regulate frequency to a specified nominal value regarding the entire network as a single area. The supplementary generation control is constructed by integrating the aggregated frequency deviation [Kundur (1994)] and hence

$$u_{\mathrm{s},[k]}(t) = \kappa_\mathrm{s} a_{[k]} \int_0^t \sum_{k\in\mathbb{N}_\mathrm{G}} \omega_{[k]}(\tau)d\tau \tag{5}$$

where κ_s denotes a feedback gain, $a_{[k]}$ denotes a scaling factor, and the aggregated frequency deviation $\sum_{k\in\mathbb{N}_\mathrm{G}} \omega_{[k]}$ is called an area control error. Further we assume that the parameters in (5) are chosen such that the entire system is stable for the case $u_{[k]} = 0$.

The model of the excitation system with AVR is given by

$$\left\{\begin{array}{ll} \dot{\boldsymbol{\eta}}_{[k]} &= \mathbf{A}_{\boldsymbol{\eta}[k]}\boldsymbol{\eta}_{[k]} + \mathbf{B}_{\boldsymbol{\eta}[k]}(\|\mathbf{v}^\star_{[k]}\| - \|\mathbf{v}_{[k]}\| + u_{[k]}) \\ &\quad + \mathbf{R}_{\boldsymbol{\eta}[k]}V^\star_{\mathrm{fd},[k]} \\ V_{\mathrm{fd},[k]} &= \mathbf{C}_{\boldsymbol{\eta}[k]}\boldsymbol{\eta}_{[k]} \end{array}\right. \tag{6}$$

where $\boldsymbol{\eta}_{[k]} \in \mathbb{R}^3$ is the state of the excitation system with AVR, $\mathbf{v}^\star_{[k]}$ is the steady voltage, $V^\star_{\mathrm{fd},[k]}$ is the steady field voltage, and $u_{[k]}$ is the control input from PSS. The excitation system with AVR has the role to provide current to the synchronous machine.

By combining (3), (4), and (6), we obtain the synchronous generator model in the form of (1) where

$$\mathbf{x}_{[k]} := \mathrm{col}(\delta_{[k]}, \omega_{[k]}, \boldsymbol{\psi}_{[k]}, \boldsymbol{\zeta}_{[k]}, \boldsymbol{\eta}_{[k]}) \in \mathbb{R}^{13}, \quad k \in \mathbb{N}_\mathrm{G}$$

and $\mathbf{f}_{[k]}(\cdot,\cdot)$ and $\mathbf{g}_{[k]}(\cdot,\cdot)$ follow from (3), (4), and (6). The signal-flow diagram of this generator model is shown in Figure 1. In the generator, the measurement output is set to be

$$\mathbf{y}_{[k]} := \mathrm{col}(\omega_{[k]}, \mathbf{v}_{[k]}).$$

The specific values of the parameters of synchronous generators are shown in Appendix.

2.2. Load, PV power plant, and Non-unit Bus

In this paper, we adopt constant impedance load models [Hatipoglu et al. (2012)]. For $k \in \mathbb{N}_\mathrm{L}$, the k-th load satisfies

$$\boldsymbol{i}_{[k]} = \boldsymbol{Y}_{[k]}\boldsymbol{v}_{[k]}, \quad k \in \mathbb{N}_\mathrm{L} \tag{7}$$

where $\boldsymbol{Y}_{[k]}$ is the admittance of the load connected to the k-th bus. Consequently, the load model in the form of (1) can be described as a static system with the output (7).

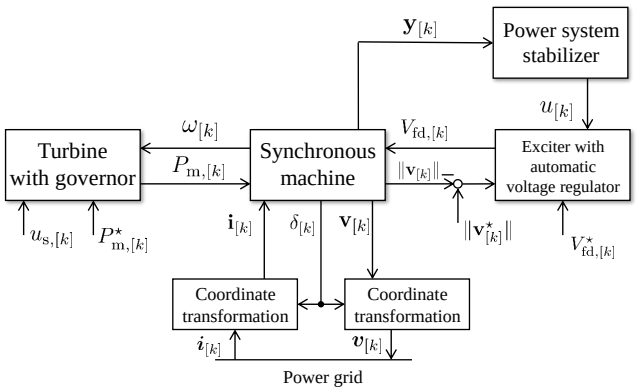

Figure 1: Signal-flow diagram of the generator model.

The model of all the PV generators inside each PV power plant is assumed to be identical for simplicity, and the total power injected from the PV power plant is obtained by summing the power output of the individual PV generators. The individual PV generator consists of a PV panel, a direct current (DC) /DC converter with a maximum power point tracking (MPPT) controller, and an inverter with a controller [Subudhi and Pradhan (2013)]. Owing to the MPPT controller, the output power of the DC/DC converter is kept constant. Because the timescale of the inverter is made sufficiently fast by the controller [Yuan et al. (2017)], one can assume that the PV generators are modeled as constant power sources. As a result, for $k \in \mathbb{N}_{\mathrm{P}}$, the k-th PV power plant satisfies

$$\boldsymbol{i}^{*}_{[k]}\boldsymbol{v}_{[k]} = \boldsymbol{p}^{\mathrm{const}}_{[k]}, \quad k \in \mathbb{N}_{\mathrm{P}} \tag{8}$$

where $\boldsymbol{p}^{\mathrm{const}}_{[k]}$ is a constant of the generated power. The PV power plant model in the form of (1) can be described as a static system.

For $k \in \mathbb{N}_{\mathrm{N}}$, the k-th non-unit bus must satisfy Kirchhoff's law, i.e., the sum of the current flowing the transmission lines connecting to the non-unit bus must be zero. The current of the non-unit bus satisfies

$$\boldsymbol{i}_{[k]} = \boldsymbol{0}, \quad k \in \mathbb{N}_{\mathrm{N}}. \tag{9}$$

The non-unit bus model in the form of (1) can be described as a static system with the output (9).

2.3. System Description

Let us suppose that there exist multiple independent system operators (ISOs) in the power grid and each component is managed by one of the ISOs. Let $\mathbb{L}$ be the index set of ISOs and $\mathcal{I}_l$ be the index of the managed components by the l-th ISO and then

$$\bigcup_{l\in\mathbb{L}} \mathcal{I}_l = \mathbb{N},$$

holds under the assumption that there is no overlap.

Let $\Sigma^{(\mathrm{nl})}_l$ be the nonlinear dynamics of the components managed by the l-th ISO. The dynamics $\Sigma^{(\mathrm{nl})}_l$ can be described as

$$\Sigma^{(\mathrm{nl})}_l : \begin{cases} \dot{\mathbf{x}}_l = \mathbf{f}_l(\mathbf{x}_l, \boldsymbol{v}_l, \boldsymbol{i}_l, \mathbf{u}_{\mathrm{s},l}, \mathbf{u}_l) \\ \boldsymbol{0} = \mathbf{g}_l(\mathbf{x}_l, \boldsymbol{v}_l, \boldsymbol{i}_l) \\ \mathbf{y}_l = \mathbf{h}_l(\mathbf{x}_l, \boldsymbol{v}_l, \boldsymbol{i}_l) \end{cases} \tag{10}$$

where

$$\begin{aligned} &\mathbf{x}_l := \mathrm{col}(\mathbf{x}_{[k]})_{k\in\mathcal{I}_l}, \quad \boldsymbol{v}_l := \mathrm{col}(\boldsymbol{v}_{[k]})_{k\in\mathcal{I}_l}, \\ &\boldsymbol{i}_l := \mathrm{col}(\boldsymbol{i}_{[k]})_{k\in\mathcal{I}_l}, \quad \mathbf{u}_{\mathrm{s},l} := \mathrm{col}(u_{\mathrm{s},[k]})_{k\in\mathcal{I}_l}, \\ &\mathbf{u}_l := \mathrm{col}(u_{\mathrm{s},[k]})_{k\in\mathcal{I}_l}, \quad \mathbf{y}_l := \mathrm{col}(\mathbf{y}_{[k]})_{k\in\mathcal{I}_l}, \end{aligned}$$

and $\mathbf{f}_l$ and $\mathbf{g}_l$ correspond to the dynamics of the components managed by the l-th ISO. From (2), $\boldsymbol{i}_l$ can be represented as

$$\boldsymbol{i}_l = \sum_{m\in\mathcal{N}_l} \boldsymbol{Y}_{lm}\boldsymbol{v}_m \tag{11}$$

where $\mathcal{N}_l$ is the neighborhood of the components managed by the l-th ISO and $\boldsymbol{Y}_{lm}$ is the corresponding admittance matrix. With (11), (10) can be described as

$$\Sigma^{(\mathrm{nl})}_l : \begin{cases} \dot{\mathbf{x}}_l = \mathbf{f}_l\left(\mathbf{x}_l, \boldsymbol{v}_l, \sum_{m\in\mathcal{N}_l}\boldsymbol{Y}_{lm}\boldsymbol{v}_m, \mathbf{u}_{\mathrm{s},l}, \mathbf{u}_l\right) \\ \boldsymbol{0} = \mathbf{g}_l\left(\mathbf{x}_l, \boldsymbol{v}_l, \sum_{m\in\mathcal{N}_l}\boldsymbol{Y}_{lm}\boldsymbol{v}_m\right) \\ \mathbf{y}_l = \mathbf{h}_l\left(\mathbf{x}_l, \boldsymbol{v}_l, \sum_{m\in\mathcal{N}_l}\boldsymbol{Y}_{lm}\boldsymbol{v}_m\right) \end{cases} \tag{12}$$

By linearizing the system (12) around an equilibrium point, we obtain the following linear model

$$\Sigma_l : \begin{cases} \dot{\mathbf{x}}_l = \mathbf{A}_l\mathbf{x}_l + \mathbf{L}_l\sum_{m\in\mathcal{N}_l}\boldsymbol{Y}_{lm}\boldsymbol{v}_m + \mathbf{B}_{\mathrm{s},l}\mathbf{u}_{\mathrm{s},l} + \mathbf{B}_l\mathbf{u}_l \\ \boldsymbol{0} = \boldsymbol{\Gamma}_l\mathbf{x}_l + \boldsymbol{\Lambda}_l\sum_{m\in\mathcal{N}_l}\boldsymbol{Y}_{lm}\boldsymbol{v}_m \\ \mathbf{y}_l = \mathbf{C}_l\mathbf{x}_l + \mathbf{D}_l\sum_{m\in\mathcal{N}_l}\boldsymbol{Y}_{lm}\boldsymbol{v}_m. \end{cases} \tag{13}$$

We treat the linear model (13) in the following discussion.

Our aim in this paper is to design PSSs that improve the damping performance against faults in the power grid. Since, in practice, it is almost impossible to obtain the whole system model, we do not assume that the complete system model of the entire system is available. Instead, it is assumed that only the model information of the subsystem of interest is available for design of the corresponding local controllers. The controller design under the model information restriction is called distributed design [Langbort and Delvenne (2010)].

One simple approach of distributed design is to apply a standard controller design technique, e.g., $\mathcal{H}_2$ optimal control, for the subsystem of interest by regarding the grid as a single-machine infinite-bus system [Wang and Swift (1997)]. However, as seen in the numerical simulation in Section 4, the entire system is possibly destabilized by the simple approach. Therefore, a systematic approach for the controller design method is crucial. In the next section, we propose a design procedure for effective PSSs that theoretically guarantee the entire system stability and improve damping performance based on retrofit control.

3. PSS Design via Retrofit Control

In this section, we first mathematically formulate the PSS design problem mentioned in the previous section. Next, we briefly review the theory of retrofit control that is the key to solving the formulated problem. We finally propose a PSS design method based on retrofit control.

3.1. Problem Formulation

The objective of each ISO is to enhance damping performance of each corresponding system against possible faults. More specifically, let $\mathcal{X}_l$ be the set of possible initial value variations of x_l. We consider designing a controller that generates u_l such that

$$\|\mathbf{x}_{\mathbb{L}}(t)\|_{\mathcal{L}_2} \leq \gamma \varepsilon_l, \quad \forall l \in \mathbb{L} \tag{14}$$

for any $\mathbf{x}_l(0) \in \mathcal{X}_l$ and $\mathbf{x}_{\mathbb{L}}(0) = [\mathbf{0}^\mathsf{T} \ \cdots \ \mathbf{x}_l(0)^\mathsf{T} \ \cdots \ \mathbf{0}^\mathsf{T}]^\mathsf{T}$ where

$$\mathbf{x}_{\mathbb{L}} := \mathrm{col}(\mathbf{x}_l)_{l \in \mathbb{L}}, \tag{15}$$

ε_l is a given desired control criterion, and $\gamma > 0$ is an independent constant of $\mathbf{u}_l$. It should be notable that local initial deflection is considered for the l-th ISO.

For controller implementation we place a restriction that the local measurement signal y_l, the interconnection signals $\{\boldsymbol{v}_m\}_{m \in \mathcal{N}_l}$, and the supplementary control input $u_{\mathrm{s},l}$ alone can be utilized as feedback signals to generate the control input u_l of PSS. In other words, each control input of PSS can be represented as

$$\mathbf{u}_l = \mathcal{K}_l(\mathbf{y}_l, \{\boldsymbol{v}_m\}_{m \in \mathcal{N}_l}, \mathbf{u}_{\mathrm{s},l}), \quad l \in \mathbb{L} \tag{16}$$

with a controller $\mathcal{K}_l$. Furthermore, for controller design we place another restriction that each controller $\mathcal{K}_l$ is designed depending only on their corresponding system parameters, namely, the elements of the set

$$\Theta_l := \{\mathbf{A}_l, \mathbf{B}_{\mathrm{s},l}, \mathbf{B}_l, \mathbf{C}_l, \mathbf{D}_l, \mathbf{L}_l, \boldsymbol{\Gamma}_l, \boldsymbol{\Lambda}_l, \{\boldsymbol{Y}_{lm}\}_{m \in \mathcal{N}_l}\}.$$

On the basis of the formulations above, we address the following problem.

Problem: Consider the network system composed of Σ_l for $l \in \mathbb{L}$ whose dynamics is given by (13). Assume that the system is stable (13) when $\mathbf{u}_l = 0$ for any $l \in \mathbb{L}$. Find $\mathcal{K}_l$ in (16) for $l \in \mathbb{L}$ such that the following requirements are satisfied:

1. The closed-loop system composed of $\{\Sigma_l\}_{l \in \mathbb{L}}$ in (13) and $\{\mathcal{K}_l\}_{l \in \mathbb{L}}$ in (16) is stable.
2. The performance criterion (14) is satisfied.
3. Each control input can be represented as (16).
4. Each controller $\mathcal{K}_l$ is designed based only on their corresponding system parameters of Θ_l.

3.2. Overview of Retrofit Control

In this subsection we briefly review the theory of retrofit control [Ishizaki et al. (2018)] that is the key to solving the formulated problem.

We first show the important lemma for the following discussion.

Lemma 1. *For the system*

$$\begin{cases} \dot{\mathbf{x}} = \mathbf{A}\mathbf{x} + \mathbf{B}\mathbf{u}_0 + \hat{\mathbf{B}}\mathbf{u} \\ \mathbf{y} = \mathbf{C}\mathbf{x}, \end{cases} \tag{17}$$

consider the system

$$\begin{cases} \dot{\hat{\boldsymbol{\xi}}} = \hat{\mathbf{A}}\hat{\boldsymbol{\xi}} + \hat{\mathbf{B}}\hat{\mathbf{w}} \\ \dot{\boldsymbol{\xi}} = \mathbf{A}\boldsymbol{\xi} + (\mathbf{A} - \hat{\mathbf{A}})\hat{\boldsymbol{\xi}} + \mathbf{B}\mathbf{w} \end{cases} \tag{18}$$

where $\hat{\mathbf{A}}$ is an arbitrary matrix whose size is compatible with $\mathbf{A}$. Assume $\mathbf{x}(0) = \boldsymbol{\xi}(0) + \hat{\boldsymbol{\xi}}(0)$ and $\mathbf{u}_0 = \mathbf{w}$ and $\mathbf{u} = \hat{\mathbf{w}}$ then

$$\mathbf{x}(t) = \boldsymbol{\xi}(t) + \hat{\boldsymbol{\xi}}(t), \quad \forall t \geq 0 \tag{19}$$

holds for any inputs $\mathbf{w}$ and $\hat{\mathbf{w}}$.

Proof: Taking the sum of the upper and lower part of (18) yields

$$\dot{\boldsymbol{\xi}}(t) + \dot{\hat{\boldsymbol{\xi}}}(t) = \mathbf{A}\left(\boldsymbol{\xi}(t) + \hat{\boldsymbol{\xi}}(t)\right) + \mathbf{B}\mathbf{w} + \hat{\mathbf{B}}\hat{\mathbf{w}}.$$

From the assumption on the initial value, (19) holds. □

Lemma 1 indicates that the state of the system (17) can be represented as the sum of the states $\boldsymbol{\xi}$ and $\hat{\boldsymbol{\xi}}$ of the system (18). Based on Lemma 1, stability and performance analysis on $\mathbf{x}$ can be reduced to that on $\boldsymbol{\xi}$ and $\hat{\boldsymbol{\xi}}$.

We assume that a controller for $\mathbf{w} = \mathbf{u}_0$ is implemented in advance and the controller can be represented as

$$\begin{cases} \dot{\boldsymbol{\xi}}_{\mathrm{c}} = \mathbf{A}_{\mathrm{c}}\boldsymbol{\xi}_{\mathrm{c}} + \mathbf{B}_{\mathrm{c}}\mathbf{y} \\ \qquad = \mathbf{A}_{\mathrm{c}}\boldsymbol{\xi}_{\mathrm{c}} + \mathbf{B}_{\mathrm{c}}\mathbf{C}(\boldsymbol{\xi} + \hat{\boldsymbol{\xi}}) \\ \mathbf{w} = \mathbf{C}_{\mathrm{c}}\boldsymbol{\xi}_{\mathrm{c}} + \mathbf{D}_{\mathrm{c}}\mathbf{y} \\ \qquad = \mathbf{C}_{\mathrm{c}}\boldsymbol{\xi}_{\mathrm{c}} + \mathbf{D}_{\mathrm{c}}\mathbf{C}(\boldsymbol{\xi} + \hat{\boldsymbol{\xi}}), \end{cases} \tag{20}$$

where the subscript c denotes "controller." Then the dynamics of $\boldsymbol{\xi}$ and $\boldsymbol{\xi}_{\mathrm{c}}$ can be given by

$$\begin{bmatrix} \dot{\boldsymbol{\xi}} \\ \dot{\boldsymbol{\xi}}_{\mathrm{c}} \end{bmatrix} = \mathbf{A}_{\mathrm{CL}} \begin{bmatrix} \boldsymbol{\xi} \\ \boldsymbol{\xi}_{\mathrm{c}} \end{bmatrix} + \mathbf{R}_0\hat{\boldsymbol{\xi}}$$

where

$$\mathbf{A}_{\mathrm{CL}} := \begin{bmatrix} \mathbf{A} + \mathbf{B}\mathbf{D}_{\mathrm{c}}\mathbf{C} & \mathbf{B}\mathbf{C}_{\mathrm{c}} \\ \mathbf{B}_{\mathrm{c}}\mathbf{C} & \mathbf{A}_{\mathrm{c}} \end{bmatrix}, \ \mathbf{R}_0 := \begin{bmatrix} \mathbf{A} - \hat{\mathbf{A}} + \mathbf{B}\mathbf{D}_{\mathrm{c}}\mathbf{C} \\ \mathbf{B}_{\mathrm{c}}\mathbf{C} \end{bmatrix}$$

and the subscript CL denotes "closed-loop." We next show the lemma for controller design to guarantee the stability of the system (18).

Lemma 2. *Assume that* $\mathbf{A}_{\rm CL}$ *is a stable matrix. Consider the controller*

$$\kappa : \left\{ \begin{array}{l} \dot{\hat{\boldsymbol{\xi}}}_{\rm c} = \hat{\mathbf{A}}_{\rm c}\hat{\boldsymbol{\xi}}_{\rm c} + \hat{\mathbf{B}}_{\rm c}\hat{\mathbf{C}}\hat{\boldsymbol{\xi}} \\ \hat{\mathbf{w}} = \hat{\mathbf{C}}_{\rm c}\hat{\boldsymbol{\xi}}_{\rm c} + \hat{\mathbf{D}}_{\rm c}\hat{\mathbf{C}}\hat{\boldsymbol{\xi}} \end{array} \right. \tag{21}$$

where $\hat{\mathbf{C}} := \mathbf{C}$*. If the matrix*

$$\hat{\mathbf{A}}_{\rm CL} := \left[\begin{array}{cc} \hat{\mathbf{A}} + \hat{\mathbf{B}}\hat{\mathbf{D}}_{\rm c}\hat{\mathbf{C}} & \hat{\mathbf{B}}\hat{\mathbf{C}}_{\rm c} \\ \hat{\mathbf{B}}_{\rm c}\hat{\mathbf{C}} & \hat{\mathbf{A}}_{\rm c} \end{array} \right]$$

is stable, then the closed-loop system (18) *with the controllers* (20) *and* (21) *is stable.*

Proof: The closed-loop system is written by

$$\left[\begin{array}{c} \dot{\boldsymbol{\xi}} \\ \dot{\hat{\boldsymbol{\xi}}}_{\rm c} \\ \dot{\boldsymbol{\xi}} \\ \dot{\boldsymbol{\xi}}_{\rm c} \end{array} \right] = \left[\begin{array}{cc} \hat{\mathbf{A}}_{\rm CL} & \left[\begin{array}{cc} \mathbf{O} & \mathbf{O} \\ \mathbf{O} & \mathbf{O} \end{array} \right] \\ \left[\begin{array}{ccc} \mathbf{R}_0 & \mathbf{O} & \mathbf{O} \end{array} \right] & \mathbf{A}_{\rm CL} \end{array} \right] \left[\begin{array}{c} \hat{\boldsymbol{\xi}} \\ \hat{\boldsymbol{\xi}}_{\rm c} \\ \boldsymbol{\xi} \\ \boldsymbol{\xi}_{\rm c} \end{array} \right].$$

Since the matrix is block triangle, we have

$$\begin{aligned} &\sigma\left(\left[\begin{array}{cc} \hat{\mathbf{A}}_{\rm CL} & \left[\begin{array}{cc} \mathbf{O} & \mathbf{O} \\ \mathbf{O} & \mathbf{O} \end{array} \right] \\ \left[\begin{array}{ccc} \mathbf{R}_0 & \mathbf{O} & \mathbf{O} \end{array} \right] & \mathbf{A}_{\rm CL} \end{array} \right] \right) \\ &= \sigma(\hat{\mathbf{A}}_{\rm CL}) \cup \sigma(\mathbf{A}_{\rm CL}). \end{aligned}$$

From the assumption that $\mathbf{A}_{\rm CL}$ is stable, the closed-loop system is stable. □

Lemma 2 indicates that the system (18) with the controller (20) is stabilized by the controller (21) if the controller (21) stabilizes the upper part of (18) under the assumption that the system (17) with (20) is stable. In other words, the stability of the cascaded system is guaranteed by the controllers that stabilize the dynamics only of $\hat{\boldsymbol{\xi}}$. Consequently, if the control input generated by κ can be obtained then the original state $\mathbf{x}$ can be stabilized by using the input, because x can be expressed as the sum of $\boldsymbol{\xi}$ and $\hat{\boldsymbol{\xi}}$. A specific methodology to create the control input of κ will be discussed in the next subsection.

We finally show the following lemma on control performance.

Lemma 3. *Assume that* $\hat{\mathbf{A}}_{\rm CL}$ *is stable and set* $\hat{\boldsymbol{\xi}}(0) = x(0)$ *and* $\boldsymbol{\xi}(0) = 0$*. With the controller* (21)*, the* $\mathcal{L}_2$*-norm of* $\mathbf{x}$ *can be evaluated as*

$$\|\mathbf{x}(t)\|_{\mathcal{L}_2} \leq \gamma_0 \hat{\varepsilon}$$

where

$$\begin{aligned} \gamma_0 &:= \|[\mathbf{I}\ \mathbf{O}](s\mathbf{I} - \mathbf{A}_{\rm CL})^{-1}\mathbf{R}_0 + \mathbf{I}\|_{\mathcal{H}_\infty}, \\ \hat{\varepsilon} &:= \|e^{\hat{\mathbf{A}}_{\rm CL}t}\hat{\boldsymbol{\xi}}(0)\|_{\mathcal{L}_2}. \end{aligned}$$

Proof: Let $\mathbf{x}(s), \boldsymbol{\xi}(s)$, and $\hat{\boldsymbol{\xi}}(s)$ be the Laplace-transformed functions of $\mathbf{x}(t), \boldsymbol{\xi}(t)$, and $\hat{\boldsymbol{\xi}}(t)$. From Lemma 1, the inequality

$$\begin{aligned} \|\mathbf{x}(t)\|_{\mathcal{L}_2} &= \|\mathbf{x}(s)\|_{\mathcal{H}_2} \\ &= \|\boldsymbol{\xi}(s) + \hat{\boldsymbol{\xi}}(s)\|_{\mathcal{H}_2} \\ &= \|[\mathbf{I}\ \mathbf{O}](s\mathbf{I} - \mathbf{A}_{\rm CL})^{-1}\mathbf{R}_0\hat{\boldsymbol{\xi}}(s) + \hat{\boldsymbol{\xi}}(s)\|_{\mathcal{H}_2} \\ &\leq \gamma_0 \|\hat{\boldsymbol{\xi}}(s)\|_{\mathcal{H}_2} \\ &= \gamma_0 \hat{\varepsilon} \end{aligned}$$

holds. □

Note that γ_0 is independent of the controller and $\hat{\varepsilon}$ depends only on $\hat{\mathbf{A}}_{\rm CL}$. From this fact we see that the $\mathcal{L}_2$-norm of the state is improved in the sense of the upper bound by designing a controller that can be designed only with $\hat{\mathbf{A}}, \hat{\mathbf{B}}$, and $\hat{\mathbf{C}}$ and makes $\hat{\varepsilon}$ small.

3.3. Proposed PSS Design Procedure

In [Ishizaki et al. (2018)], a controller design method that satisfies the requirements of Problem has been proposed for the following system

$$\left\{ \begin{array}{l} \dot{\mathbf{x}}_l = \mathbf{A}_l\mathbf{x}_l + \mathbf{B}_l\mathbf{u}_l + \mathbf{L}_l \sum_{m \in \mathcal{N}_l} \mathbf{Y}_{lm}\mathbf{v}_m \\ \mathbf{v}_l = \boldsymbol{\Gamma}_l\mathbf{x}_l \\ \mathbf{y}_l = \mathbf{C}_l\mathbf{x}_l. \end{array} \right.$$

On the other hand, the dynamics of each synchronous generator has feedthrough terms in the outputs as shown in (13) and the existing method in [Ishizaki et al. (2018)] cannot be directly applied to the power system. In this subsection, we extend the result in [Ishizaki et al. (2018)] to power grids and give a solution to Problem.

We first consider designing κ in (21). From (13), we have

$$\boldsymbol{v}_{\mathbb{L}} = \boldsymbol{\Pi}_{\mathbb{L}}\mathbf{x}_{\mathbb{L}} \tag{22}$$

where $x_{\mathbb{L}}$ is the states of the whole system defined by (15), and

$$\begin{aligned} &\boldsymbol{v}_{\mathbb{L}} := {\rm col}(\boldsymbol{v}_l)_{l \in \mathbb{L}}, \quad \boldsymbol{\Pi}_{\mathbb{L}} := -(\boldsymbol{\Lambda}_{\mathbb{L}}\boldsymbol{Y}_{\mathbb{L}})^{-1}\boldsymbol{\Gamma}_{\mathbb{L}}, \\ &\boldsymbol{\Lambda}_{\mathbb{L}} := {\rm diag}(\boldsymbol{\Lambda}_l)_{l \in \mathbb{L}}, \quad \boldsymbol{\Gamma}_{\mathbb{L}} := {\rm diag}(\boldsymbol{\Gamma}_l)_{l \in \mathbb{L}}. \end{aligned}$$

Substituting (22) to (13), we obtain the entire system model

$$\Sigma_{\mathbb{L}} : \left\{ \begin{array}{rl} \dot{\mathbf{x}}_{\mathbb{L}} &= \mathbf{A}_{\mathbb{L}}x_{\mathbb{L}} + \mathbf{B}_{{\rm s},\mathbb{L}}\mathbf{u}_{{\rm s},\mathbb{L}} + \mathbf{B}_{\mathbb{L}}\mathbf{u}_{\mathbb{L}} \\ \mathbf{y}_{\mathbb{L}} &= \mathbf{C}_{\mathbb{L}}\mathbf{x}_{\mathbb{L}} \\ \dot{\mathbf{x}}_{\rm s} &= \mathbf{C}_{\rm s}\mathbf{x}_{\mathbb{L}} \\ \mathbf{u}_{{\rm s},\mathbb{L}} &= \kappa_{\rm s}\mathbf{a}\mathbf{x}_{\rm s} \end{array} \right. \tag{23}$$

where

$$\begin{aligned} &\mathbf{u}_{\mathbb{L}} := {\rm col}(\mathbf{u}_l)_{l \in \mathbb{L}}, \quad \mathbf{y}_{\mathbb{L}} := {\rm col}(\mathbf{y}_l)_{l \in \mathbb{L}}, \\ &\mathbf{A}_{\mathbb{L}} := {\rm diag}(\mathbf{A}_{\mathbf{l}})_{l \in \mathbb{L}} + \mathbf{L}_{\mathbb{L}}\boldsymbol{Y}_{\mathbb{L}}\boldsymbol{\Pi}_{\mathbb{L}}, \\ &\mathbf{B}_{\mathbb{L}} := {\rm diag}(\mathbf{B}_l)_{l \in \mathbb{L}}, \quad \mathbf{B}_{{\rm s},\mathbb{L}} := {\rm diag}(\mathbf{B}_{{\rm s},l})_{l \in \mathbb{L}}, \\ &\mathbf{L}_{\mathbb{L}} := {\rm diag}(\mathbf{L}_{\mathbf{l}})_{l \in \mathbb{L}}, \\ &\mathbf{C}_{\mathbb{L}} := {\rm diag}(\mathbf{C}_l)_{l \in \mathbb{L}} + \mathbf{D}_{\mathbb{L}}\boldsymbol{Y}_{\mathbb{L}}\boldsymbol{\Pi}_{\mathbb{L}}, \\ &\mathbf{D}_{\mathbb{L}} := {\rm diag}(\mathbf{D}_l)_{l \in \mathbb{L}}, \end{aligned} \tag{24}$$

$\mathbf{x}_{\rm s}$ is the state of the supplementary controller, $\mathbf{C}_{\rm s}$ is the matrix associated with the aggregated frequency deviation, $\mathbf{a} := {\rm col}(a_{[k]})_{k \in \mathbb{N}_{\rm g}}$, and $\mathbf{u}_{{\rm s},\mathbb{L}} := {\rm col}(\mathbf{u}_{{\rm s},l})_{l \in \mathbb{L}}$.

Let us decide matrices $\mathbf{A}_{{\rm c},l}, \mathbf{B}_{{\rm c},l}, \mathbf{C}_{{\rm c},l}, \mathbf{D}_{{\rm c},l}$ for $l \in \mathbb{L}$ so as to satisfy

$$\|e^{\hat{\mathbf{A}}_{{\rm CL},l}t}\mathbf{x}_l(0)\|_{\mathcal{L}_2} \leq \varepsilon_l, \quad \forall \mathbf{x}_l(0) \in \mathcal{X}_l \tag{25}$$

where

$$\hat{\mathbf{A}}_{{\rm CL},l} := \left[\begin{array}{cc} \mathbf{A}_l + \mathbf{B}_l\mathbf{D}_{{\rm c},l}\mathbf{C}_l & \mathbf{B}_l\mathbf{C}_{{\rm c},l} \\ \mathbf{B}_{{\rm c},l}\mathbf{C}_l & \mathbf{A}_{{\rm c},l} \end{array} \right].$$

This design problem becomes a standard $\mathcal{H}_2$ suboptimal control problem that is easy to solve. We here show the following theorem.

Theorem 1. *For the system* (13)*, design* κ_l *so as to satisfy* (25)*. Define* $\hat{\mathbf{A}}, \hat{\mathbf{B}}$*, and* $\hat{\mathbf{C}}$ *as*

$$\hat{\mathbf{A}}_{\mathbb{L}} := \mathrm{diag}(\mathbf{A}_l)_{l\in\mathbb{L}}, \quad \hat{\mathbf{B}}_{\mathbb{L}} := \mathrm{diag}(\mathbf{B}_l)_{l\in\mathbb{L}},$$
$$\hat{\mathbf{C}}_{\mathbb{L}} := \mathrm{diag}(\mathbf{C}_l)_{l\in\mathbb{L}},$$

set

$$\gamma := \|[\mathbf{I}\ \mathbf{O}](s\mathbf{I} - \mathbf{A}_{\mathbb{L},\mathrm{CL}})^{-1}\mathbf{R} + \mathbf{I}\|_{\mathcal{H}_\infty}$$

where

$$\mathbf{A}_{\mathbb{L},\mathrm{CL}} := \begin{bmatrix} \mathbf{A}_{\mathbb{L}} & \mathbf{B}_{\mathrm{s},\mathbb{L}}\kappa_{\mathrm{s}}\mathbf{a} \\ \mathbf{C}_{\mathrm{s}} & \mathbf{O} \end{bmatrix}, \quad \mathbf{R} := \begin{bmatrix} \mathbf{A}_{\mathbb{L}} - \hat{\mathbf{A}}_{\mathbb{L}} \\ \mathbf{C}_{\mathrm{s}} \end{bmatrix},$$

and design the controller (21) *by*

$$\mathbf{A}_{\mathrm{c}} := \mathrm{diag}(\mathbf{A}_{\mathrm{c},l})_{l\in\mathbb{L}}, \quad \mathbf{B}_{\mathrm{c}} := \mathrm{diag}(\mathbf{B}_{\mathrm{c},l})_{l\in\mathbb{L}}$$
$$\mathbf{C}_{\mathrm{c}} := \mathrm{diag}(\mathbf{C}_{\mathrm{c},l})_{l\in\mathbb{L}}, \quad \mathbf{D}_{\mathrm{c}} := \mathrm{diag}(\mathbf{D}_{\mathrm{c},l})_{l\in\mathbb{L}}.$$

Then the performance criterion (14) *is satisfied.*

Proof: Since $\hat{\boldsymbol{\xi}}(0) = \mathbf{x}(0)$,

$$\|e^{\hat{\mathbf{A}}_{\mathrm{cl}}t}\hat{\boldsymbol{\xi}}(0)\|_{\mathcal{L}_2} = \sum_{l\in\mathbb{L}} \|e^{\hat{\mathbf{A}}_{\mathrm{CL},l}t}\mathbf{x}_l(0)\|_{\mathcal{L}_2}.$$

Therefore, for any $\mathbf{x}_l(0) \in \mathcal{X}_l$,

$$\|e^{\hat{\mathbf{A}}_{\mathrm{CL}}t}\hat{\boldsymbol{\xi}}(0)\|_{\mathcal{L}_2} = \|e^{\hat{\mathbf{A}}_{\mathrm{CL},l}t}\mathbf{x}_l(0)\|_{\mathcal{L}_2}$$

holds for $\mathbf{x}(0) = [\mathbf{0}^{\mathsf{T}}\ \cdots\ \mathbf{x}_l(0)^{\mathsf{T}}\ \cdots\ \mathbf{0}^{\mathsf{T}}]^{\mathsf{T}}$. From Lemma 3, we have

$$\begin{aligned}\|\mathbf{x}_{\mathbb{L}}(t)\|_{\mathcal{L}_2} &\le \gamma|e^{\hat{\mathbf{A}}_{\mathrm{CL}}t}\hat{\boldsymbol{\xi}}(0)\|_{\mathcal{L}_2} \\ &= \gamma\|e^{\hat{\mathbf{A}}_{\mathrm{CL},l}t}\mathbf{x}_l(0)\|_{\mathcal{L}_2}.\end{aligned}$$

From the assumption, for any $\mathbf{x}_l(0) \in \mathcal{X}_l$,

$$\|\mathbf{x}(t)\|_{\mathcal{L}_2} \le \gamma\varepsilon_l$$

holds. □

Theorem 1 gives a design policy for $\mathbf{A}_{\mathrm{c},l}, \mathbf{B}_{\mathrm{c},l}, \mathbf{C}_{\mathrm{c},l}, \mathbf{D}_{\mathrm{c},l}$ such that the performance criterion is satisfied. Following the above procedure, we can design κ_l under the distributed design restriction.

We next consider implementation of the designed controllers. Because the input is $\hat{\mathbf{C}}\hat{\boldsymbol{\xi}}$ in (21) and $\hat{\boldsymbol{\xi}}$ is a virtual variable, the signal cannot be utilized as a measurement signal even if the entire state $\mathbf{x}_{\mathbb{L}}$ can be measured. To tackle this problem, by the coordinate transformation

$$\begin{bmatrix} \mathbf{x}_{\mathbb{L}} \\ \hat{\mathbf{x}}_{\mathbb{L}} \end{bmatrix} = \begin{bmatrix} \mathbf{I} & \mathbf{I} \\ \mathbf{O} & \mathbf{I} \end{bmatrix} \begin{bmatrix} \hat{\boldsymbol{\xi}} \\ \boldsymbol{\xi} \end{bmatrix} \tag{26}$$

we consider the system

$$\begin{cases} \dot{\mathbf{x}}_{\mathbb{L}} &= \mathbf{A}_{\mathbb{L}}\mathbf{x}_{\mathbb{L}} + \mathbf{B}_{\mathrm{s},\mathbb{L}}\mathbf{u}_{\mathrm{s},\mathbb{L}} + \mathbf{B}_{\mathbb{L}}\mathbf{u}_{\mathbb{L}} \\ \dot{\mathbf{x}}_{\mathrm{s}} &= \mathbf{C}_{\mathrm{s}}\mathbf{x}_{\mathbb{L}} \\ \mathbf{u}_{\mathrm{s},\mathbb{L}} &= \kappa_{\mathrm{s}}\mathbf{a}\mathbf{x}_{\mathrm{s}} \\ \dot{\hat{\mathbf{x}}}_{\mathbb{L}} &= \hat{\mathbf{A}}_{\mathbb{L}}\hat{\mathbf{x}}_{\mathbb{L}} + (\mathbf{A}_{\mathbb{L}} - \hat{\mathbf{A}}_{\mathbb{L}})\mathbf{x}_{\mathbb{L}} + \mathbf{B}_{\mathrm{s},\mathbb{L}}\mathbf{u}_{\mathrm{s},\mathbb{L}}. \end{cases} \tag{27}$$

By the inverse of the coordinate transformation (26), $\hat{\boldsymbol{\xi}} = \mathbf{x}_{\mathbb{L}} - \hat{\mathbf{x}}_{\mathbb{L}}$ holds. Hence if $\hat{\mathbf{x}}_{\mathbb{L}}$ in (27) can be generated in a distributed manner then the control input in (21) can be generated by using $\hat{\mathbf{x}}_{\mathbb{L}}$. We call a system that generates $\hat{\mathbf{x}}$ an *output rectifier* and consider designing and implementing a distributed output rectifier.

Notice that

$$\mathbf{A}_{\mathbb{L}} - \hat{\mathbf{A}}_{\mathbb{L}} = \mathbf{L}_{\mathbb{L}}\boldsymbol{Y}_{\mathbb{L}}\boldsymbol{\Pi}_{\mathbb{L}}.$$

Because $\mathbf{A}_{\mathbb{L}} - \hat{\mathbf{A}}_{\mathbb{L}}$ does not have block diagonal structure and $(\mathbf{A}_{\mathbb{L}} - \hat{\mathbf{A}}_{\mathbb{L}})\mathbf{x}_{\mathbb{L}}$ cannot be generated from $\mathbf{x}_{\mathbb{L}}$ in a distributed manner, a distributed output rectifier that generates $\hat{\mathbf{x}}_{\mathbb{L}}$ using $\mathbf{x}_{\mathbb{L}}$ cannot be designed and implemented. To avoid this issue, consider using not the state $\mathbf{x}_{\mathbb{L}}$ but the interconnection signal $\boldsymbol{v}_{\mathbb{L}}$. Note the relationship

$$\begin{aligned}(\mathbf{A}_{\mathbb{L}} - \hat{\mathbf{A}}_{\mathbb{L}})\mathbf{x}_{\mathbb{L}} &= \mathbf{L}_{\mathbb{L}}\boldsymbol{Y}_{\mathbb{L}}\boldsymbol{\Pi}_{\mathbb{L}}\mathbf{x}_{\mathbb{L}} \\ &= \mathbf{L}_{\mathbb{L}}\boldsymbol{Y}_{\mathbb{L}}\boldsymbol{v}_{\mathbb{L}} \\ &= \mathrm{col}\left(\mathbf{L}_l \textstyle\sum_{m\in\mathcal{N}_l} \boldsymbol{Y}_{lm}\boldsymbol{v}_m\right)_{l\in\mathbb{L}}.\end{aligned} \tag{28}$$

We then have the following theorem employing the relationship (28).

Theorem 2. *Consider the systems* (27) *and*

$$\begin{cases} \dot{\mathbf{x}}_{\mathbb{L}} &= \mathbf{A}_{\mathbb{L}}\mathbf{x}_{\mathbb{L}} + \mathbf{B}_{\mathrm{s},\mathbb{L}}\mathbf{u}_{\mathrm{s},\mathbb{L}} + \mathbf{B}_{\mathbb{L}}\mathbf{u}_{\mathbb{L}} \\ \dot{\mathbf{x}}_{\mathrm{s}} &= \mathbf{C}_{\mathrm{s}}\mathbf{x}_{\mathbb{L}} \\ \mathbf{u}_{\mathrm{s},\mathbb{L}} &= \kappa_{\mathrm{s}}\mathbf{a}\mathbf{x}_{\mathrm{s}} \\ \dot{\hat{\mathbf{x}}}_l &= \mathbf{A}_l\hat{\mathbf{x}}_l + \mathbf{L}_l\textstyle\sum_{m\in\mathcal{N}_l}\boldsymbol{Y}_{lm}\boldsymbol{v}_m + \mathbf{B}_{\mathrm{s},l}\mathbf{u}_{\mathrm{s},l}, \quad l \in \mathbb{L}. \end{cases}$$

Set the initial values $\hat{\mathbf{x}}_{\mathbb{L}}(0) = 0, \hat{\mathbf{x}}_l(0) = 0, l \in \mathbb{L}$ *and then for any* $\mathbf{u}_{\mathbb{L}}$

$$\hat{\mathbf{x}}_{\mathbb{L}}(t) = \mathrm{col}(\hat{\mathbf{x}}_l(t))_{l\in\mathbb{L}}, \quad \forall t \ge 0$$

holds.

Proof: Define the error signal by $\hat{\mathbf{e}} := \hat{\mathbf{x}}_{\mathbb{L}} - \mathrm{col}(\hat{\mathbf{x}}_l)_{l\in\mathbb{L}}$. From (22), (24), and (28), we have

$$\dot{\hat{\mathbf{e}}} = \hat{\mathbf{A}}_{\mathbb{L}}\hat{\mathbf{e}}.$$

From the initial conditions, $\hat{\mathbf{e}}(t) = 0$ for any $t \ge 0$. Hence, $\hat{\mathbf{x}}_{\mathbb{L}}(t) = \mathrm{col}(\hat{\mathbf{x}}_l(t))_{l\in\mathbb{L}}$ for any $t \ge 0$. □

From Theorem 2, the output rectifier

$$\mathcal{C}_l : \begin{cases} \dot{\hat{\mathbf{x}}}_l = \mathbf{A}_l\hat{\mathbf{x}}_l + \mathbf{L}_l\textstyle\sum_{m\in\mathcal{N}_l}\boldsymbol{Y}_{lm}\boldsymbol{v}_m + \mathbf{B}_{\mathrm{s},l}\mathbf{u}_{\mathrm{s},l}, \\ \hat{\mathbf{y}}_l = \mathbf{y}_l - (\mathbf{C}_l\hat{\mathbf{x}}_l + \mathbf{D}_l\textstyle\sum_{m\in\mathcal{N}_l}\boldsymbol{Y}_{lm}\boldsymbol{v}_m), \end{cases} \quad l \in \mathbb{L} \tag{29}$$

can create the signal

$$\begin{aligned}\hat{\mathbf{C}}\hat{\boldsymbol{\xi}} &= \hat{\mathbf{C}}(\mathbf{x}_{\mathbb{L}} - \mathrm{col}(\hat{\mathbf{x}}_l)_{l\in\mathbb{L}}) \\ &= \hat{\mathbf{y}}_{\mathbb{L}}\end{aligned}$$

where $\hat{\mathbf{y}}_{\mathbb{L}} := \mathrm{col}(\hat{\mathbf{y}}_l)_{l\in\mathbb{L}}$ and generate the control input in (21).

At last, under the initial conditions $\mathbf{x}(0) = \hat{\boldsymbol{\xi}}(0)$, $\boldsymbol{\xi}(0) = 0$, $\hat{\mathbf{x}}_l(0) = 0, l \in \mathbb{L}$, letting $\mathbf{A} = \mathbf{A}_{\mathbb{L}}, \mathbf{B} = \mathbf{B}_{\mathrm{s},\mathbb{L}}, \hat{\mathbf{B}} = \mathbf{B}_{\mathbb{L}}$,

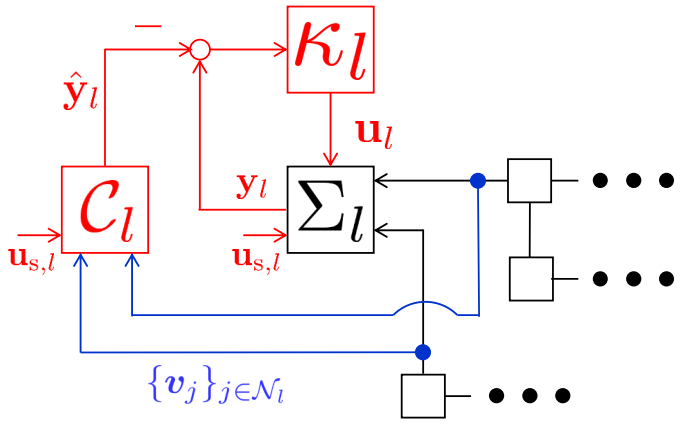

Figure 2: Block diagram of the local system structure composed of $\Sigma_l, \mathcal{C}_l$, and κ_l.

and $\mathbf{C} = \mathbf{C}_{\mathbb{L}}$ we have an equivalent system composed of $\Sigma_l, \mathcal{C}_l, \kappa_l, l \in \mathbb{L}$ to the closed-loop system (18) with (21), where Σ_l is given by (13), $\mathcal{C}_l$ is given by (29), and

$$\kappa_l : \left\{ \begin{array}{l} \dot{\mathbf{x}}_{\mathrm{c},l} = \mathbf{A}_{\mathrm{c},l}\mathbf{x}_{\mathrm{c},l} + \mathbf{B}_{\mathrm{c},l}\hat{\mathbf{y}}_l \\ \mathbf{u}_{\mathrm{l},l} = \mathbf{C}_{\mathrm{c},l}\mathbf{x}_{\mathrm{c},l} + \mathbf{D}_{\mathrm{c},l}\hat{\mathbf{y}}_l \end{array} \right., \quad l \in \mathbb{L}. \tag{30}$$

It is seen that κ_l can be designed only with the parameters $\mathbf{A}_l, \mathbf{B}_l, \mathbf{C}_l$, and $\mathbf{D}_l$ from (25) and $\mathcal{C}_l$ and κ_l can be designed and implemented in a distributed manner from (29) and (30). Figure 2 illustrates the block diagram associated with $\Sigma_l, \mathcal{C}_l$, and κ_l.

Summarizing the discussion above, we finally reach a solution to Problem. Design the parameters $\mathbf{A}_{\mathrm{c},l}, \mathbf{B}_{\mathrm{c},l}, \mathbf{C}_{\mathrm{c},l}$, and $\mathbf{D}_{\mathrm{c},l}$ so as to satisfy (25). Construct the controller $\mathcal{K}_l(\mathbf{y}_l, \{\boldsymbol{v}_m\}_{m\in\mathcal{N}_l}, \mathbf{u}_{\mathrm{s},l})$ as

$$\mathcal{K}_l : \left\{ \begin{array}{l} \mathcal{C}_l : \left\{ \begin{array}{l} \dot{\hat{\mathbf{x}}}_l = \mathbf{A}_l\hat{\mathbf{x}}_l + \mathbf{L}_l \sum_{m\in\mathcal{N}_l} \boldsymbol{Y}_{lm}\boldsymbol{v}_m + \mathbf{B}_{\mathrm{s},l}\mathbf{u}_{\mathrm{s},l} \\ \hat{\mathbf{y}}_l = \mathbf{y} - (\mathbf{C}_l\hat{\mathbf{x}}_l + \mathbf{D}_l \sum_{m\in\mathcal{N}_l} \boldsymbol{Y}_{lm}\boldsymbol{v}_m) \end{array} \right. \\ \kappa_l : \left\{ \begin{array}{l} \dot{\mathbf{x}}_{\mathrm{c},l} = \mathbf{A}_{\mathrm{c},l}\mathbf{x}_{\mathrm{c},l} + \mathbf{B}_{\mathrm{c},l}\hat{\mathbf{y}}_l \\ \mathbf{u}_{\mathrm{c},l} = \mathbf{C}_{\mathrm{c},l}\mathbf{x}_{\mathrm{c},l} + \mathbf{D}_{\mathrm{c},l}\hat{\mathbf{y}}_l. \end{array} \right. \end{array} \right. \tag{31}$$

It can be confirmed that the requirements of Problem are satisfied as follows.

1. Since the system with the supplementary controller is stable, Lemma 2 indicates the stability of the closed-loop system.
2. From the equivalence between the obtained closed-loop system and the system (18) with (21), Theorem 1 implies that (14) holds.
3. The controller (31) utilizes only $\mathbf{y}_l, \{\boldsymbol{v}_m\}_{m\in\mathcal{N}_l}$, and $\mathbf{u}_{\mathrm{s},l}$.
4. From the form of $\mathcal{C}_l$ and the design procedure of κ_l, every controller can be designed in a distributed manner only with the local parameters in Θ_l.

4. Simulation

In this section, we confirm that the proposed retrofit control effectively works to enhance damping performance of power grids. We consider the PV-integrated EAST30 model, which is a benchmark model of the bulk power system in the eastern half of Japan, shown in Figure 3. The grid consists of 137 buses, 30 generators, 31 loads, 30 PVs, and a transmission network connecting the components. The tie-line parameters of this EAST30 model is shown in [The Institute of Electrical Engineers of Japan Power and Energy (2016)]. The original IEEJ EAST30 model does not contain any PV power plants and we introduce PV power plants to simulate future power grids. We decide the places of the PV power plants based on the data that indicate the regions for future PV power plants of Japan [Ministry of Economy, Trade, and Industry (2017b)]. Each generator is 13-dimensional. Consequently the entire system is 390-dimensional. We assume that the PV output covers 6% of the total demand. The PV amount corresponds to the case where 30% of the FIT introduced amount in Japan is penetrated. The parameters of the supplementary control are determined as

$$\kappa_{\mathrm{s}} = -1, \quad a_{[k]} = 1, \quad \forall k \in \mathbb{N}_{\mathrm{G}}.$$

Note that the system is stable with the supplementary control provided that no primary control is added.

Let

$$\begin{array}{l} \mathbb{L} = \{1, 2\}, \\ \mathcal{I}_1 \cap \mathbb{N}_{\mathrm{G}} = \{1, \ldots, 5\}, \\ \mathcal{I}_1 \cap \mathbb{N}_{\mathrm{L}} = \{37, 40, 41, 42, 44\}, \\ \mathcal{I}_1 \cap \mathbb{N}_{\mathrm{P}} = \{112, 117, 122, 127, 132\}, \\ \mathcal{I}_1 \cap \mathbb{N}_{\mathrm{N}} = \{31, \ldots, 36, 38, 39, 43, 50, \ldots, 58, 60, \ldots, 68\}, \\ \mathcal{I}_2 = \{1, \ldots, N\} \setminus \mathcal{I}_1. \end{array}$$

Suppose that a fault happens in the second generator and the effect of the fault is modeled by an impulsive disturbance of the angle of the generator, that is,

$$\mathbf{x}_{[k],0} = \left\{ \begin{array}{ll} 0.1\mathbf{e}_1 & \text{if } k = 2, \\ \mathbf{0} & \text{otherwise.} \end{array} \right.$$

To guarantee the stability we apply the proposed retrofit control to the power system. The primary controller (30) for $\mathcal{I}_1$ is designed based on $\mathcal{H}_2$ optimal control to minimize

$$J_1 := \int_0^\infty \left(\mathbf{x}_1^{\mathsf{T}}\mathbf{Q}_1\mathbf{x}_1 + r\mathbf{u}_1^{\mathsf{T}}\mathbf{u}_1\right) dt$$

where

$$\mathbf{Q}_1 = q_{\delta,1}\hat{\mathbf{e}}_1\hat{\mathbf{e}}_1^{\mathsf{T}} + q_{\omega,1}\hat{\mathbf{e}}_2\hat{\mathbf{e}}_2^{\mathsf{T}} + q_1\mathbf{I}$$

and $\hat{\mathbf{e}}_i := \mathbf{1}_{|\mathcal{I}_1\cap\mathbb{N}_{\mathrm{G}}|} \otimes \mathbf{e}_i$, $\mathbf{1}_M$ is the M-dimensional all-ones vector, $\otimes$ is the Kronecker product, $\mathbf{e}_i \in \mathbb{R}^{13}$ for $i \in \{1, 2\}$ is the canonical basis associated with the i-th coordination, and $q_{\delta,1}, q_{\omega,1}, q_1$ and r are positive scalar values. Note that $q_{\delta,1}$ and $q_{\omega,1}$ correspond to the angle and the frequency, respectively. On the other hand, we suppose that the primary controller for $\mathcal{I}_2$ is not added to the original system. All simulations have been performed with MATPOWER [Zimmerman et al. (2011)] on `MATLAB`.

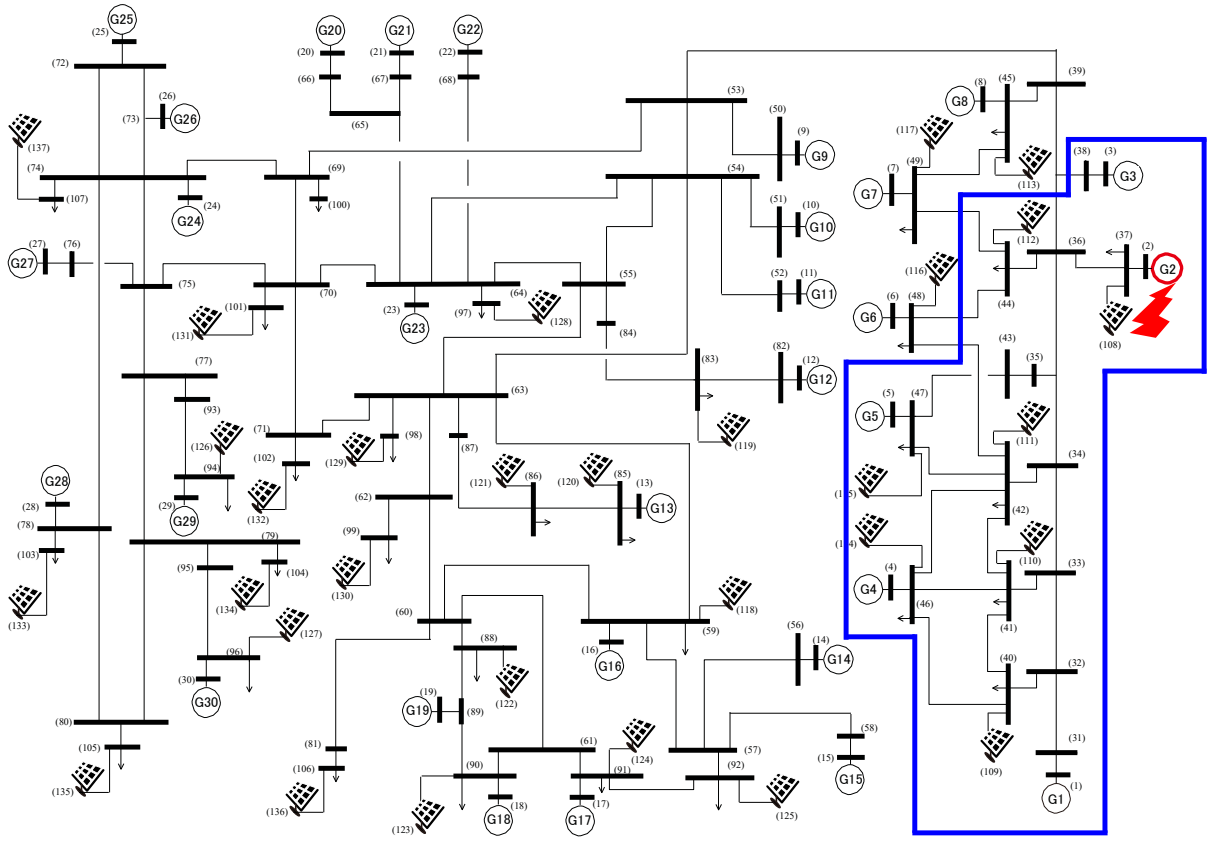

Figure 3: PV-integrated IEEJ EAST 30-machine power system.

Figure 4 shows the free responses of all generators' frequency deviation for $t \in [0, 50]$. Figure 5 shows the responses with the controller designed based on the single-machine infinite-bus system for $t \in [0, 1.5]$ and it can be observed that the system becomes unstable. On the other hand, Figure 6 shows the responses of the closed-loop system with the proposed method, where $q_1, q_{\delta,1}$ are set to be 1 and 10^3, and the weight for control input $r = 1$ and the weight for frequencies $q_{\omega,1} = 10^7 (=: q_{\omega,0})$. We can see from the figure that the entire system stability is preserved by our proposed method. Moreover, as shown in Figure 7 that illustrates the responses for $t \in [0, 0.5]$, the peak value is reduced to the value -0.0753 by the proposed method while the original peak value is -0.0904. To further mitigate the peak value, we change the weight for frequencies by $q_{\omega,1} = q_{\omega,0} \times 10^3$ and show the result in Figure 8. As shown in Figure 9, the peak value is reduced to the value -0.0505, which is 55% of the original peak value. This result shows the effectiveness of our proposed retrofit control for power system stabilization.

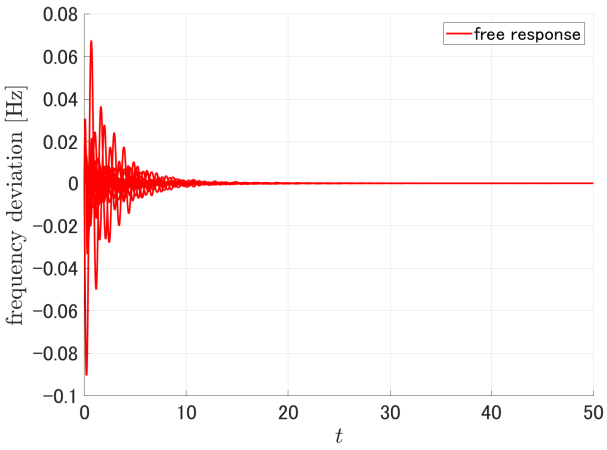

Figure 4: Free responses of all generators' frequencies.

5. Conclusion

In this paper, we have proposed a distributed design methods for PSSs to improve damping performance of PV-integrated power grids via retrofit control. Because power systems into which large amount of PV is pene-

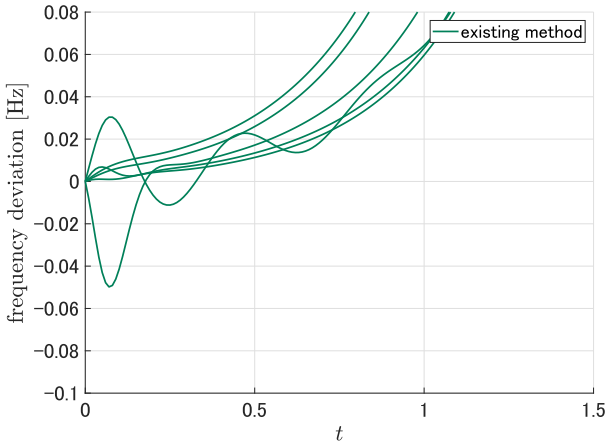

Figure 5: Responses of all generators' frequencies with the controller designed based on the single-machine infinite-bus system.

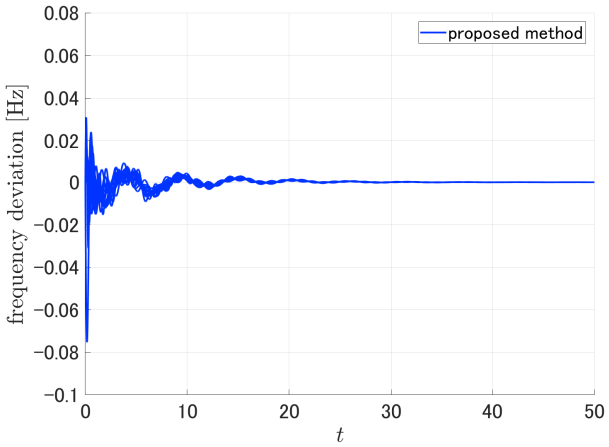

Figure 6: Responses of all generators' frequencies of the closed-loop system with the proposed method when $q_{\omega,1} = q_{\omega,0}$.

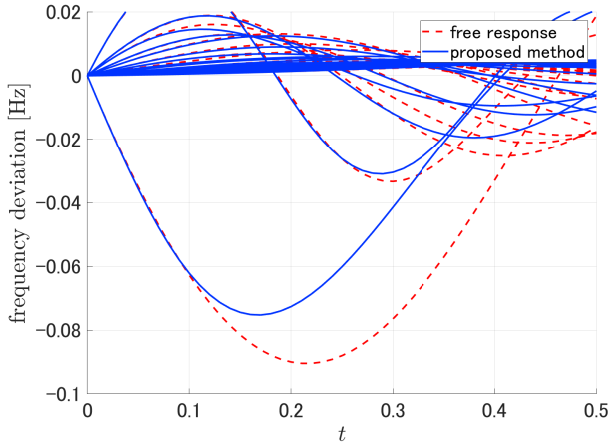

Figure 7: Comparison of the responses without control and with the proposed method when $q_{\omega,1} = q_{\omega,0}$.

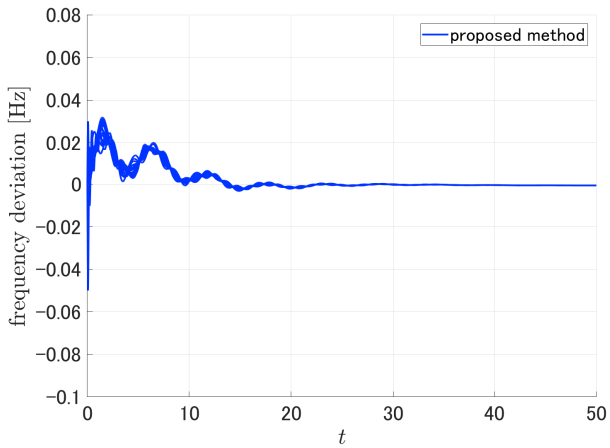

Figure 8: Responses of all generators' frequencies of the closed-loop system with the proposed method when $q_{\omega,1} = q_{\omega,0} \times 10^3$.

trated are susceptible to disturbance and easily destabilized, it is required to develop a novel method for designing PSS that ensures the stability of the entire system on the premise of distributed design. While existing practical methods, such as single-machine infinite-bus based approaches, do not achieve theoretical assurance of the stability, retrofit control is a promising approach to fulfill the requirements. The proposed method is an extension of the existing retrofit control to be applicable for power systems. Numerical examples in the simulation through EAST30 show that the proposed method not only stabilizes the power system, which can be destabilized by a conventional method based on the single-machine infinite-bus model, but also enhances the damping performance. Future works include robust controller design with consideration of modeling error. Another important future work is to verify the applicability of the proposed method to more general future power grids that contain other distributed energy resources, such as energy storage.

Acknowledgement

This research was supported by JST CREST Grant Number JPMJCR15K1, Japan. The authors are deeply grateful to Yoshifumi Zouka from Hiroshima University, Chiaki Kojima from Toyama Prefectural University, Masaki Inoue from Keio University, Kengo Urata and Fumiya Watanabe from Tokyo Institute of Technology for their help with the numerical simulations.

Appendix

We give the specific expression of the dynamics of the synchronous generators. We consider three kinds of synchronous generator, namely, thermal power generators, nuclear power generators, and hydroelectric power generators. The subscript $k \in \mathbb{N}_{\mathrm{G}}$ is omitted for simplicity.

The matrices of the synchronous machine expressed

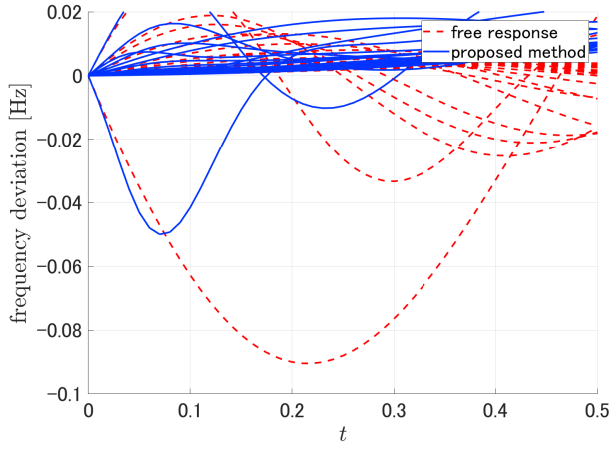

Figure 9: Comparison of the responses without control and with the proposed method when $q_{\omega,1} = q_{\omega,0} \times 10^3$.

as (3) are given by

$$\mathbf{A}_{\psi} = \begin{bmatrix} \frac{-(1+\gamma_d)}{T'_{do}} & \frac{K_d\gamma_d}{T'_{do}} & 0 & 0 \\ \frac{1}{K_d T''_{do}} & \frac{-1}{T''_{do}} & 0 & 0 \\ 0 & 0 & \frac{-(1+\gamma_q)}{T'_{qo}} & \frac{K_q\gamma_q}{T'_{qo}} \\ 0 & 0 & \frac{1}{K_q T''_{qo}} & \frac{-1}{T''_{qo}} \end{bmatrix},$$

$$\mathbf{B}_{\psi} = \begin{bmatrix} -\frac{(X_d - X'_d)(X''_d - X_l)}{T'_{do}(X'_d - X_l)} & 0 \\ -\frac{X'_d - X_l}{K_d T''_{do}} & 0 \\ 0 & \frac{(X_q - X'_q)(X''_q - X_l)}{T'_{qo}(X'q - X_l)} \\ 0 & \frac{X'_q - X_l}{K_q T''_{qo}} \end{bmatrix},$$

$$\mathbf{B}_V = [1/T'_{do}\ 0\ 0\ 0]^\top,$$

$$\mathbf{C}_{\psi} = \begin{bmatrix} 0 & 0 & \frac{X''_q - X_l}{X'_q - X_l} & K_q \frac{X'_q - X''_q}{X'_q - X_l} \\ \frac{X''_d - X_l}{X'_d - X_l} & K_d \frac{X'_d - X''_d}{X'_d - X_l} & 0 & 0 \end{bmatrix},$$

$$\mathbf{D}_{\psi} = \begin{bmatrix} 0 & X''_q \\ -X''_d & 0 \end{bmatrix},$$

$$\gamma_\circ = \frac{(X_\circ - X'_\circ)(X'_\circ - X''_\circ)}{(X'_\circ - X_l)^2},$$

$$K_\circ = 1 + \frac{(X'_\circ - X_l)(X''_\circ - X_l)}{(X'_\circ - X''_\circ)(X_\circ - X_l)}, \circ \in \{d, q\},$$

where $X_d, X'_d, X''_d, T'_{do}, T''_{do}$ are d-axis synchronous reactance, transient reactance, subtransient reactance, and transient open-circuit. $X_q, X'_q, X''_q, T'_{qo}, T''_{qo}$ are similar q-axis quantities, X_l is a stator leakage reactance (see [The Institute of Electrical Engineers of Japan (1999)] for the specific values). Note that all kinds of synchronous generator have the same parameters in terms of synchronous machine.

For thermal power generators and nuclear power generators, the matrices of the turbine with governor expressed as (4) is given by

$$\mathbf{A}_{\varsigma} = \begin{bmatrix} -5 & 0 & 0 & 0 \\ -5 & -5 & 0 & 0 \\ 0 & 4 & -4 & 0 \\ 0 & 0 & \frac{1}{9} & -\frac{1}{9} \end{bmatrix}, \quad \mathbf{B}_{\varsigma} = \begin{bmatrix} 125 \\ 0 \\ 0 \\ 0 \end{bmatrix},$$

$$\mathbf{R}_{\varsigma} = [0\ \ 5\ \ 0\ \ 0]^\top, \quad \mathbf{C}_{\varsigma} = [0\ \ 0\ \ 0.3\ \ 0.7].$$

On the other hand, for hydroelectric power generators, the dynamics of the turbine with governor is given by

$$\mathbf{A}_{\varsigma} = \begin{bmatrix} -0.01 & -0.25 & 0 & 0 \\ -\frac{1}{2000} & -\frac{2.3}{24} & 0 & 0 \\ \frac{1}{7} & 0 & -\frac{1}{7} & 0 \\ 0 & 0 & \frac{2}{3} & -\frac{2}{3} \end{bmatrix}, \quad \mathbf{B}_{\varsigma} = \begin{bmatrix} -0.25 \\ -\frac{1}{80} \\ 0 \\ 0 \end{bmatrix},$$

$$\mathbf{R}_{\varsigma} = \begin{bmatrix} 0 & 0 & \frac{1}{7} & 0 \end{bmatrix}^\top, \quad \mathbf{C}_{\varsigma} = [0\ \ 0\ \ -2\ \ 3].$$

The dynamics of the excitation system with AVR expressed as (6) is given by

$$\mathbf{A}_{\eta} = \begin{bmatrix} -5 & 0 & -5 \\ 50 & -0.5 & 0 \\ 10 & -0.1 & -2 \end{bmatrix}, \quad \mathbf{B}_{\eta} = \begin{bmatrix} 5 \\ 0 \\ 0 \end{bmatrix},$$

$$\mathbf{R}_{\eta} = \begin{bmatrix} 0 \\ 0.5 \\ 0.1 \end{bmatrix}, \quad \mathbf{C}_{\eta} = [0\ \ 1\ \ 0].$$

Note that all kinds of synchronous generator have the same parameters in terms of excitation system as synchronous machine.

For the values of the admittance matrix $\boldsymbol{Y}$, see [The Institute of Electrical Engineers of Japan (1999)].

References

Blaabjerg, F., Chen, Z., Kjaer, S.B., 2004. Power electronics as efficient interface in dispersed power generation systems. IEEE Transactions on Power Electronics 19, 1184–1194.

Blaabjerg, F., Teodorescu, R., Liserre, M., Timbus, A.V., 2006. Overview of control and grid synchronization for distributed power generation systems. IEEE Transactions on Industrial Electronics 53, 1398–1409.

Blaabjerg, F., Yang, Y., Yang, D., Wang, X., 2017. Distributed power-generation systems and protection. Proceedings of the IEEE 105, 1311–1331.

Dörfler, F., Jovanović, M.R., Chertkov, M., Bullo, F., 2014. Sparsity-promoting optimal wide-area control of power networks. IEEE Transactions on Power Systems 29, 2281–2291.

Eftekharnejad, S., Vittal, V., Heydt, G.T., Keel, B., Loehr, J., 2013. Impact of increased penetration of photovoltaic generation on power systems. IEEE Trans. Power Syst. 28, 893–901.

Etemadi, A.H., Davison, E.J., Iravani, R., 2012. A decentralized robust control strategy for multi-DER microgrids; Part I: Fundamental concepts. IEEE Transactions on Power Delivery 27, 1843–1853.

Hatipoglu, K., Fidan, I., Radman, G., 2012. Investigating effect of voltage changes on static ZIP load model in a microgrid environment, in: 2012 North American Power Symposium (NAPS), pp. 1–5.

Ishizaki, T., Sadamoto, T., Imura, J., Sandberg, H., Johansson, K.H., 2018. Retrofit control: Localization of controller design and implementation. Automatica 95, 336–346.

Kundur, P., 1994. Power System Stability and Control. McGraw-Hill Education.

Langbort, C., Delvenne, J., 2010. Distributed design methods for linear quadratic control and their limitations. IEEE Trans. Autom. Control 55, 2085–2093.

Ministry of Economy, Trade, and Industry, 2015. Long-term energy supply and demand outlook. [Online]. Available: http://www.meti.go.jp/english/press/2015/pdf/0716_01a.pdf.

Ministry of Economy, Trade, and Industry, 2017a. Feed-in Tariffs in Japan: Five years of achievements and future challenges. [Online]. Available: https://www.renewable-ei.org/en/activities/reports/img/pdf/20170810/REI_Report_20170908_FIT5years_Web_EN.pdf.

Ministry of Economy, Trade, and Industry, 2017b. Website for information disclosure on Feed-in Tariff in Japan. [Online]. Available: http://www.enecho.meti.go.jp/category/saving_and_new/saiene/statistics/index.html (in Japanese).

Ortega, R., Galaz, M., Astolfi, A., Sun, Y., Shen, T., 2005. Transient stabilization of multimachine power systems with nontrivial transfer conductances. IEEE Transactions on Automatic Control 50, 60–75.

Sasahara, H., Ishizaki, T., Sadamoto, T., Imura, J., 2017. Distributed design of local controllers for transient stabilization in power grids, in: IFAC 2017 World Congress, pp. 5597–5602.

Subudhi, B., Pradhan, R., 2013. A comparative study on maximum power point tracking techniques for photovoltaic power systems. IEEE Transactions on Sustainable Energy 4, 89–98.

Tamimi, B., Cañizares, C., Bhattacharya, K., 2013. System stability impact of largescale and distributed solar photovoltaic generation: the case of Ontario Canada. IEEE Trans. Sustain. Energy 4, 680–688.

The Institute of Electrical Engineers of Japan, 1999. Japanese power system model. IEEJ Technical Report 754, 1–82. (in Japanese).

The Institute of Electrical Engineers of Japan Power and Energy, 2016. http://www.iee.jp/pes/?page_id=141.

Wang, H.F., Swift, F.J., 1997. A unified model for the analysis of FACTS devices in damping power system oscillations. I. Single-machine infinite-bus power systems. IEEE Transactions on Power Delivery 12, 941–946.

Yuan, H., Yuan, X., Hu, J., 2017. Modeling of grid-connected VSCs for power system small-signal stability analysis in DC-link voltage control timescale. IEEE Transactions on Power Systems 32, 3981–3991.

Zimmerman, R.D., Murillo-Sánchez, C.E., Thomas, R.J., 2011. MATPOWER: Steady-state operations, planning, and analysis tools for power systems research and education.